The role of land use change on the development and evolution of the west coast trough, convective clouds, and precipitation in southwest Australia

Udaysankar S. Nair,[1,2] Y. Wu,[1] J. Kala,[3] T. J. Lyons,[2,3] R. A. Pielke Sr.,[4] and J. M. Hacker[5]

Received 25 August 2010; revised 27 December 2010; accepted 6 January 2011; published 9 April 2011.

[1] Land clearing for agricultural purposes in southwest Australia has created a landscape where a 750 km rabbit-proof fence separates 13 million hectares of croplands from the remnant native vegetation to the east. The Bunny Fence Experiment (BuFex) was conducted in the vicinity of the intended vermin-proof boundary in December 2005 and August 2007. The experiment examined the role of land cover change (LCC) on the preferential formation of clouds over the native vegetation that often terminates along the vermin-proof fence as well as the regional rainfall reduction observed in this region. Observations and numerical model analysis show that the formation and development of the west coast trough (WCT), which is a synoptic-scale feature that initiates spring and summertime convection, is impacted by land cover change and that the cloud fields induced by the WCT would extend farther west in the absence of the LCC. The surface convergence patterns associated with the wintertime WCT circulation are substantially altered by LCC, due to changes in both WCT dynamics and surface aerodynamic roughness, leading to a rainfall decrease to the west of the rabbit fence. Although this study focuses on only two events, it further illustrates that LCC has significant regional impacts in southwest Western Australia regardless of large-scale shifts in the climate system.

Citation: Nair, U. S., Y. Wu, J. Kala, T. J. Lyons, R. A. Pielke Sr., and J. M. Hacker (2011), The role of land use change on the development and evolution of the west coast trough, convective clouds, and precipitation in southwest Australia, *J. Geophys. Res.*, *116*, D07103, doi:10.1029/2010JD014950.

1. Introduction

[2] Over the last several decades, approximately 13 million hectares of native vegetation in southwest Australia have been replaced by nonnative, rain-fed agricultural species [*Lyons et al.*, 1993]. A 750 km long rabbit-proof fence separates this wedge-shaped region of land clearing in southwest Australia from the remnant native vegetation to the east and is readily visible in satellite imagery due to enhanced albedo, with darker native vegetation found to the east of the fence and lighter agricultural regions to the west (Figure 1).

[3] Differing land cover leads to contrasting land surface characteristics on either side of the fence that vary seasonally, with the albedo and roughness length over the agricultural region during the summer being higher before harvest and lower when it is bare after harvest [*Huang et al.*, 1995; *Ray et al.*, 2003]. Whereas the albedo and surface roughness of the agricultural area decreases substantially following harvest when vegetated surface is replaced by bare soil, the native vegetation areas show very small seasonal variations in surface vegetation characteristics [*Huang et al.*, 1995; *Ray et al.*, 2003]. Rainfall observations show about a 20 percent decline of winter rainfall since the 1970s confined mainly to agricultural areas [*Pittock*, 1983; *Williams* 1991, *IOCI Panel*, 2002; *Narisma and Pitman*, 2003] (Figure 2). The rainfall decrease in this region has been attributed to large-scale changes in circulation including a shift toward the high-phase regime of the Southern Annular Mode (SAM), with increases in surface pressure over southern Australia and a poleward shift of the extratropical jet [*Pittock*, 1983; *Hope*, 2006; *Bates et al.*, 2008, *Nicholls*, 2010] resulting in a decrease of westerly winds bringing less rainfall over land [*Cai and Watterson*, 2002]. Observations of preferential cloud formation and enhanced sensible heat fluxes over native vegetation [*Lyons et al.*, 1993; *Huang et al.*, 1995; *Ray et al.*, 2003], however, suggest that effects of land cover change (LCC) may also be substantial and this has been confirmed by modeling studies. *Timbal and Arblaster* [2006] showed that LCC in southwest Western Australia (SWWA)

[1]Earth System Science Center, University of Alabama in Huntsville, Huntsville, Alabama, USA.
[2]Centre of Excellence for Climate Change Woodland and Forest Health, School of Biology and Biotechnology, Murdoch University, Murdoch, Western Australia, Australia.
[3]School of Environmental Sciences, Murdoch University, Murdoch, Western Australia, Australia.
[4]Cooperative Institute for Research in Environmental Sciences, University of Colorado at Boulder, Boulder, Colorado, USA.
[5]Airborne Research Australia, Flinders University, Adelaide, South Australia, Australia.

0148-0227/11/2010JD014950

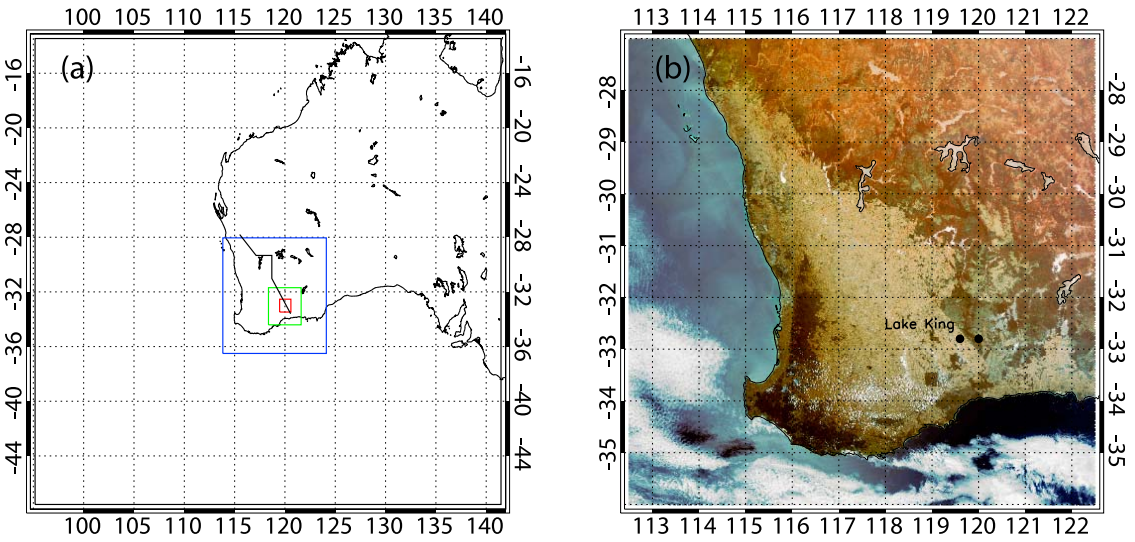

Figure 1. (a) The location of the rabbit-proof fence in the southwest Australian region and the grids used in the numerical model simulations. The first grid, with the coarsest spacing of 64 km, covers the entire region shown in Figure 1a. The second, third, and fourth grids, with grid spacing of 16, 4, and 1 km, respectively, are shown using red, green, and blue squares, respectively. (b) False color image over the second grid, derived from the data acquired by the Aqua Moderate Imaging Spectroradiometer (MODIS) sensor on 17 December 2005. Also marked on the map are the two BuFex radiosonde stations.

reinforces the negative rainfall trends due to other forcings; however, since their imposed change was larger than observed, they could not quantify the role of LCC in the observed rainfall decline. *Pitman et al.* [2004] found that the effect of reduced roughness from LCC and the associated increase in moisture divergence may be a significant contributor to a decrease in southwest Western Australian rainfall. At locations farther inland, *Pitman et al.* [2004] found that LCC induced enhanced moisture convergence and rainfall in accordance with observations [*Williams*, 1991]. However, it is noticeable that the rainfall has continued to decrease in spite of the termination of large-scale land clearing in this region. A question of relevance in this context is whether the land use change is contributing to the ongoing decrease in rainfall or if it is just modulating the severity of a larger-scale declining trend over the region.

[4] A striking visual manifestation of the impact of land use on atmospheric processes in southwest Australia are cloud fields that are observed to form preferentially over the native vegetation area in satellite imagery to the east of the rabbit-proof fence [*Lyons et al.*, 1993; *Lyons*, 2002; *Ray et al.*, 2003] (Figure 3a), with cumulus clouds occurring preferentially over the native vegetation up to 10% of the time during the austral summer [*Ray et al.*, 2003]. Based on analysis of a one-dimensional numerical model, this phenomenon is hypothesized to be due to enhanced planetary boundary layer (PBL) height over native vegetation exceeding the Lifting Condensation Level (LCL) and increasing the possibility of cloud formation over the native vegetation areas [*Lyons et al.*, 1993; *Lyons*, 2002]. Prior aircraft observations of higher sensible heat fluxes over native vegetation areas do support this hypothesis [*Lyons et al.*, 1993, 2001]. The Bunny Fence Experiments in December 2005 (BuFex05), December 2006 (BuFex06), and August 2007 (BuFex07), a continuation of series of a field campaigns in southwest Australia [*Lyons et al.*, 1993], examined this hypothesis through observations of boundary layer development as a function of land cover and season using radiosonde, aircraft and ground-based measurements. Along with numerical modeling analysis, these observations are used to show that the west coast trough (WCT), a quasi-permanent surface heat low-pressure region in northwestern Australia

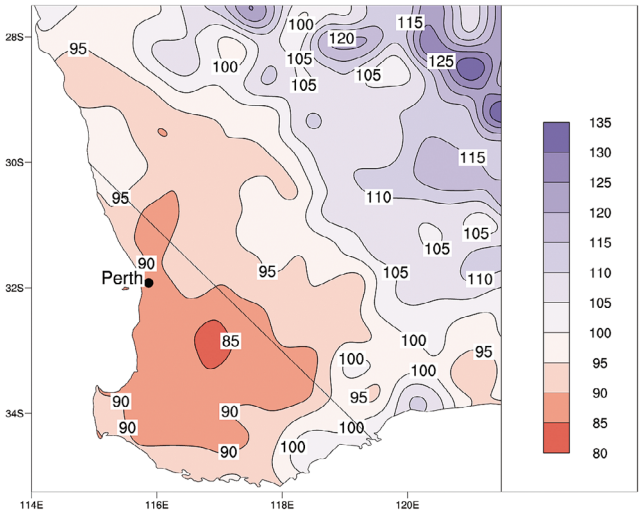

Figure 2. Average May–October rainfall over the 1976–2001 period as a percentage of the average May–October over the 1925–1975 period, from *IOCI Panel* [2002].

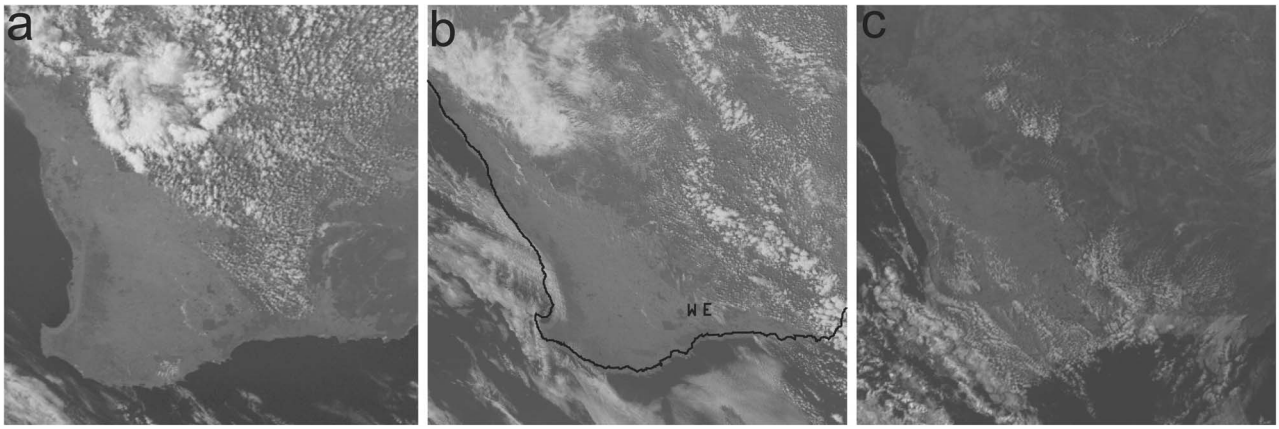

Figure 3. The 1500 LST geostationary visible channel imagery over southwest Australia for (a) 3 January 1999, (b) 18 December 2005, and (c) 13 August 2007. The imagery for 3 January 1999 is from the Geostationary Meteorological Satellite (GMS), and the imagery for the other case days are from the Multifunction Transport Satellite (MTSAT).

that forces summertime convection in southwest Australia, is impacted by LCC.

2. Data and Methods

[5] The primary goal of this study is to use observational and numerical modeling analysis of selected case studies to examine the processes through which land use change in southwest Australia impacts atmospheric processes in this region, especially the development and evolution of the WTC.

[6] Paired radiosonde releases, approximately every 3 h during the day, from locations 20 km to the west and east of the rabbit-proof fence (Figure 1) in the Lake King area of southwest Australia during December 2005 (austral summer) and August 2007 (austral winter) were used to compute planetary boundary layer height (PBL) and lifting condensation level (LCL). The PBL height is determined as the height of potential temperature or equivalent potential temperature inversion. The LCL is computed utilizing the procedure outlined by *Bolton* [1980]. The differences in PBL heights over the native vegetation and agricultural areas during the afternoon hours are used to investigate the hypothesis. For specific case days, the diurnal variation of PBL and LCL heights are analyzed to determine whether boundary layer development is vigorous enough for cloud formation to occur. The case days were selected to eliminate preferential cloudiness impacts (higher cloud cover over one site earlier during the day compared to the other side), and days in which radiosonde release was delayed, etc.

[7] Aircraft observations of heat and moisture fluxes from the native vegetation and agricultural regions are also compared to determine the cause for differences in boundary layer development between the two regions of differing land use. Surface energy fluxes from the aircraft are processed using a technique detailed by *Lyons et al.* [2001]. Only long (>30 km), low-altitude (<25 m AGL) traverses are used in

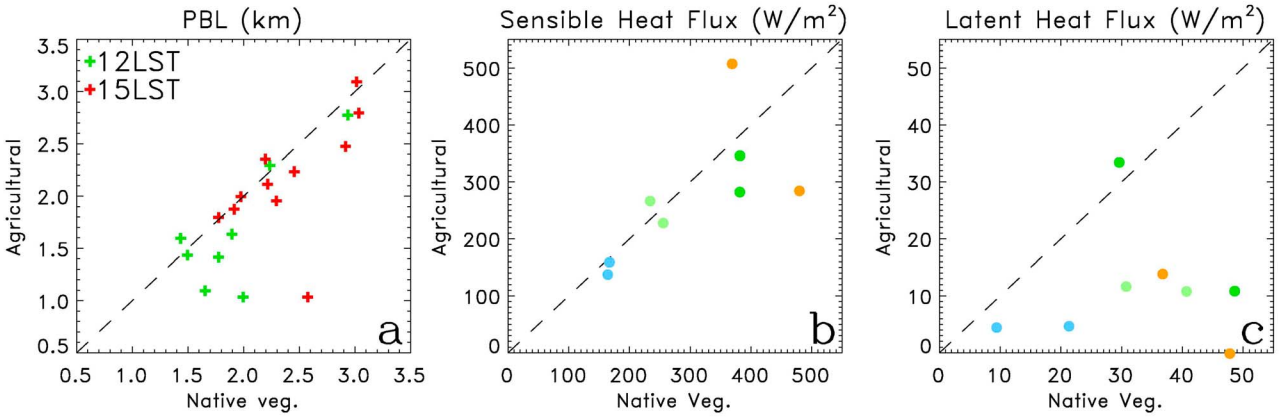

Figure 4. Comparison between native vegetation and agricultural area: (a) PBL heights (December 2005), (b) sensible heat fluxes (December 2005 and 2006), and (c) latent heat fluxes (December 2005 and 2006). The green, orange, light green, and light blue symbols in Figures 4b and 4c denote late morning (0200–0400 UTC), midday (0400–0600 UTC), midafternoon (0600–0800 UTC) and late afternoon (0800–1000 UTC) observations, respectively.

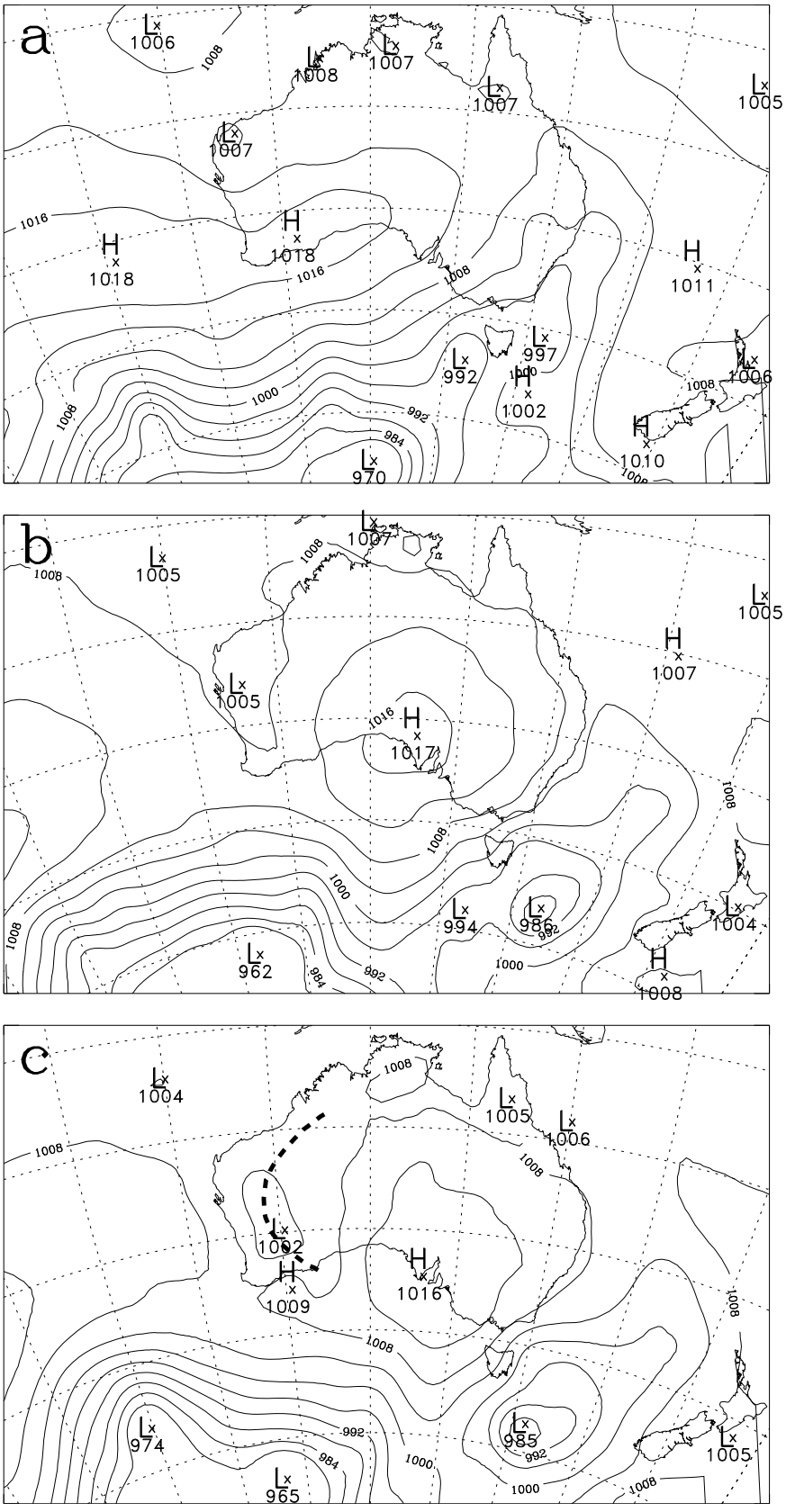

Figure 5. Surface weather chart at (a) 0800 LST (0000 UTC) 17 December 2005, (b) 0800 LST 18 December 2005, and (c) 2000 LST 18 December 2005.

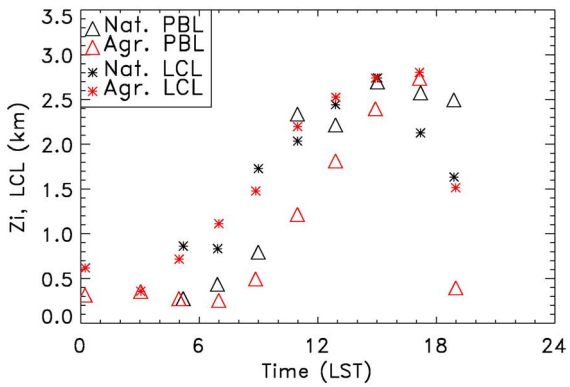

Figure 6. Time evolution of PBL height (triangle) and LCL (asterisk) and LCL (asterisk) for 17 December 2005 (red, agriculture; black, native vegetation).

the analysis. The data are detrended first and then a square Lanzcos high-pass filter is applied after which the data are separately averaged for sections of flight path over agricultural and native vegetation areas.

[8] The Regional Atmospheric Modeling System (RAMS), version 6.0 [*Cotton et al.*, 2003], is used to simulate the evolution of regional atmospheric conditions for selected case days of WCT activity, in order to understand the role of LCC on differing boundary layer evolution, cloud, and precipitation formation. The days considered in this study are 17 December 2005 and 12 August 2007 during which the WCT feature played a major role in the development of convection. A nested grid configuration consisting of four grids of 64 km, 16 km, 4 km, and 1 km grid spacing and covering a domain span in the X and Y direction of 3712 km × 3712 km, 928 km × 928 km, 296 km × 296 km, and 102 km × 102 km, respectively, is utilized in the simulations (Figure 1). In the vertical, all the grids utilize a stretched grid of 50 points and a grid stretch ratio of 1.05, with the grid spacing increasing from 10 m at the surface

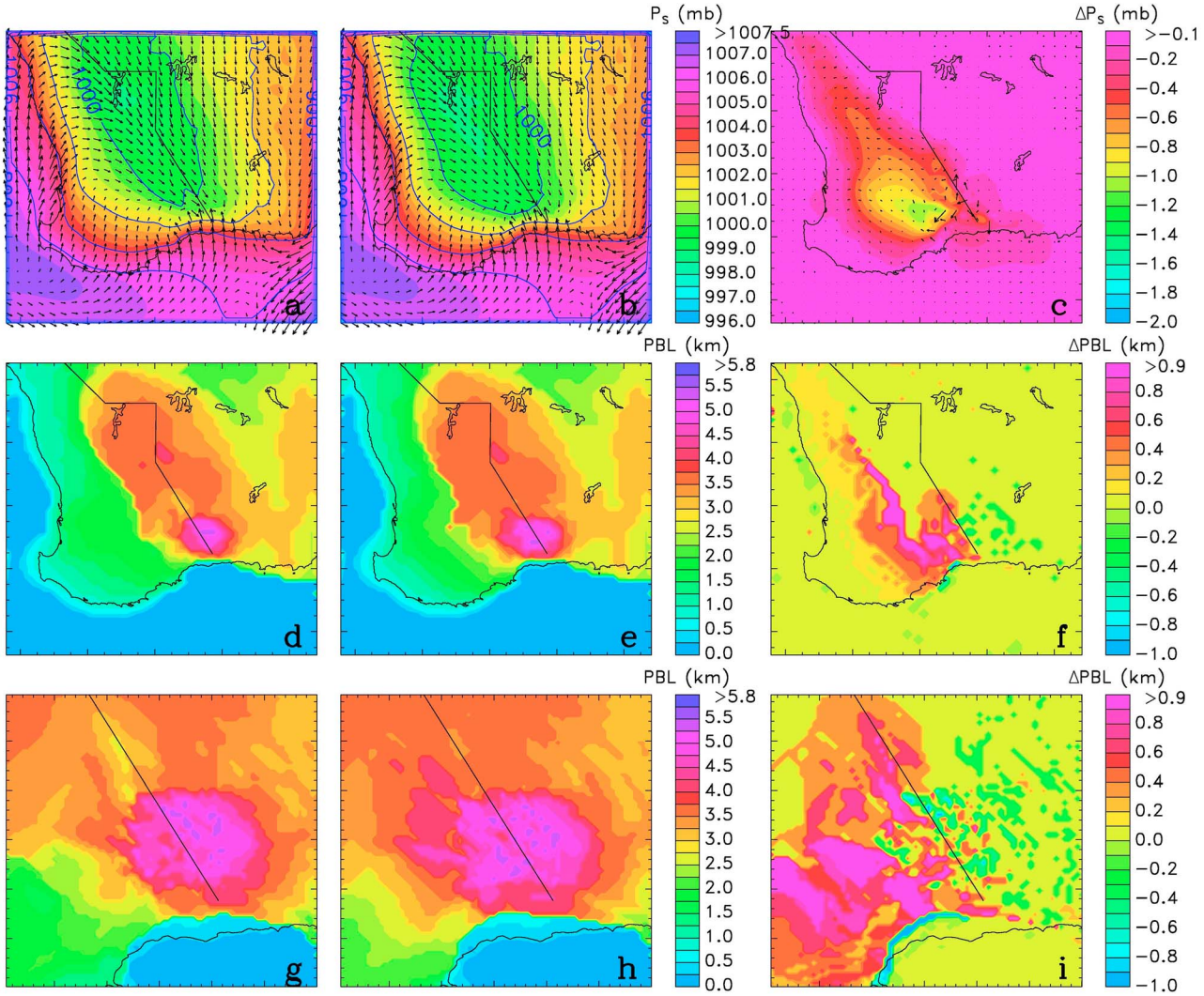

Figure 7. (a and b) The mean sea level pressure within grid 2 of CLU and PELU simulations at 0500 LST, 18 December 2005, and (c) the difference between PELU and CLU simulations. (d, e, and f) Same as Figures 7a, 7b, and 7c but for PBL heights. (g, h, and i) Same as Figures 7d, 7e, and 7f but for grid 4.

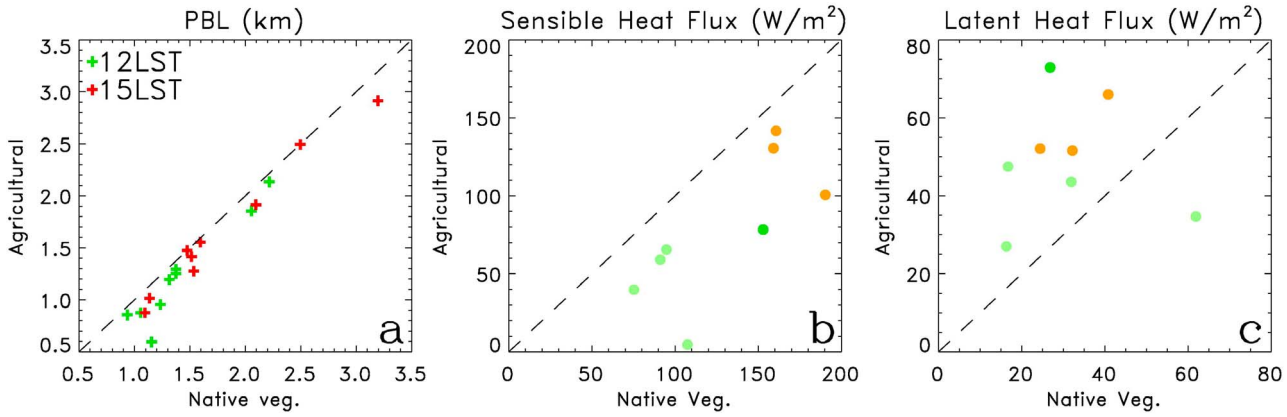

Figure 8. Comparison between native vegetation and agricultural area: (a) PBL heights (August 2007), (b) sensible heat fluxes (August 2007), and (c) latent heat fluxes (August 2007). The green, orange, and light green symbols in Figures 8b and 8c denote late morning (0200–0400 UTC), midday (0400–0600 UTC), and midafternoon (0600–0800 UTC) observations.

to 1 km higher up in the atmosphere after which it remains constant.

[9] The soil model uses 8 layers located at depths 0.1, 0.2, 0.4, 0.6, 0.8, 1.0, 1.5, and 2.0 m. The atmospheric variables in RAMS at 0 UTC is initialized using the 1° × 1° global tropospheric final analysis (FNL) created by the National Center for Environmental Prediction (NCEP). The NCEP FNL analysis is also used to specify temporally varying top and lateral boundary conditions at six-hourly intervals by nudging five grid points along the lateral boundaries and for the grid points at altitudes greater that 14 km along the top boundary toward values consistent with the NCEP FNL analysis. Explicit cloud microphysical parameterization was used on all four grids while the two outer grids also utilized convective parameterization. The two-stream radiative transfer parameterization of *Harrington et al.* [1999] was used in the simulations.

[10] Two types of experiments are conducted, assuming two differing scenarios of land use: (1) current land use (referred as CLU from hereon) conditions and (2) pre-European land use (referred as PELU from hereon) where the wedge-shaped region of agricultural clearing is replaced by native vegetation. The cumulative impact of land use change on atmospheric processes is of interest to the present study, which is examined through the comparison of the effect of CLU with that of PELU, i.e., before large-scale land clearing for agriculture. Soil moisture and soil temperatures in these simulations are initialized using corresponding fields obtained for two sets of longer-term simulations assuming CLU and PELU scenarios, initiated from the beginning of the month prior to the month in which the case day occurred. In these longer-term simulations, the initial soil moisture conditions and temperature conditions were initialized using fields obtained from the NCEP FNL soil analysis. The soil moisture and temperature fields in these simulations were allowed to continuously evolve, while the atmospheric conditions were reinitialized every 24 h. The goal of this experimental design was to maintain realistic variation of large-scale atmospheric conditions, while allowing the higher-resolution grids to develop a more realistic spatial distribution of soil moisture that is not present in the 1° × 1° analysis. The Land Ecosystem and Atmosphere Feedback (LEAF) submodel [*Walko et al.*, 2000] is utilized to simulate vegetation-atmosphere exchange. Leaf Area Index, vegetation fractional cover, vegetation albedo, and roughness height are all parameterized based on the satellite-derived Normalized Difference Vegetation Index (NDVI).

3. Results

3.1. Summertime Boundary Layer and Convective Development

[11] The near-simultaneous observations of PBL heights during the afternoon hours of December 2005 over the native vegetation and agricultural areas show consistently higher values over the native vegetation (Figure 4a), in agreement with the hypothesis proposed on the basis of one-dimensional boundary layer modeling [*Lyons*, 2002]. The majority of observations over the native vegetation show a higher PBL (5 out of 8 and 7 out of 11 at 1200 and 1500 LST, respectively; Figure 4a) that is closer to the LCL (6 out of 8 and 7 out of 11 at 1200 and 1500 LST, respectively, not shown), indicating a higher potential for cloud formation compared to the agricultural areas. The mean difference in PBL height between the native vegetation and agricultural areas is ~260 m and ~240 m at 1200 and 1500 LST, respectively. The 1200 LST difference is significant at a 95% confidence level, while the 1500 LST difference is significant only at the 90% confidence level. Aircraft measurements of near-surface energy fluxes show higher sensible heat (Figure 4b) and latent fluxes (Figure 4c) over the native vegetation areas, consistent with lower albedo and higher aerodynamic roughness over these areas [*Huang et al.*, 1995; *Ray et al.*, 2003].

[12] The radiosonde observations show that the maximum PBL height attained on the majority of BuFex field study days (~72% at 1500 LST) in December 2005 was substantially less than the LCL height at the corresponding time. However, under calm conditions that accompany the influence of a high-pressure system in the region, a heat low often develops over the Pilbara and Kimberley regions of Western Australia, eventually establishing the west coast

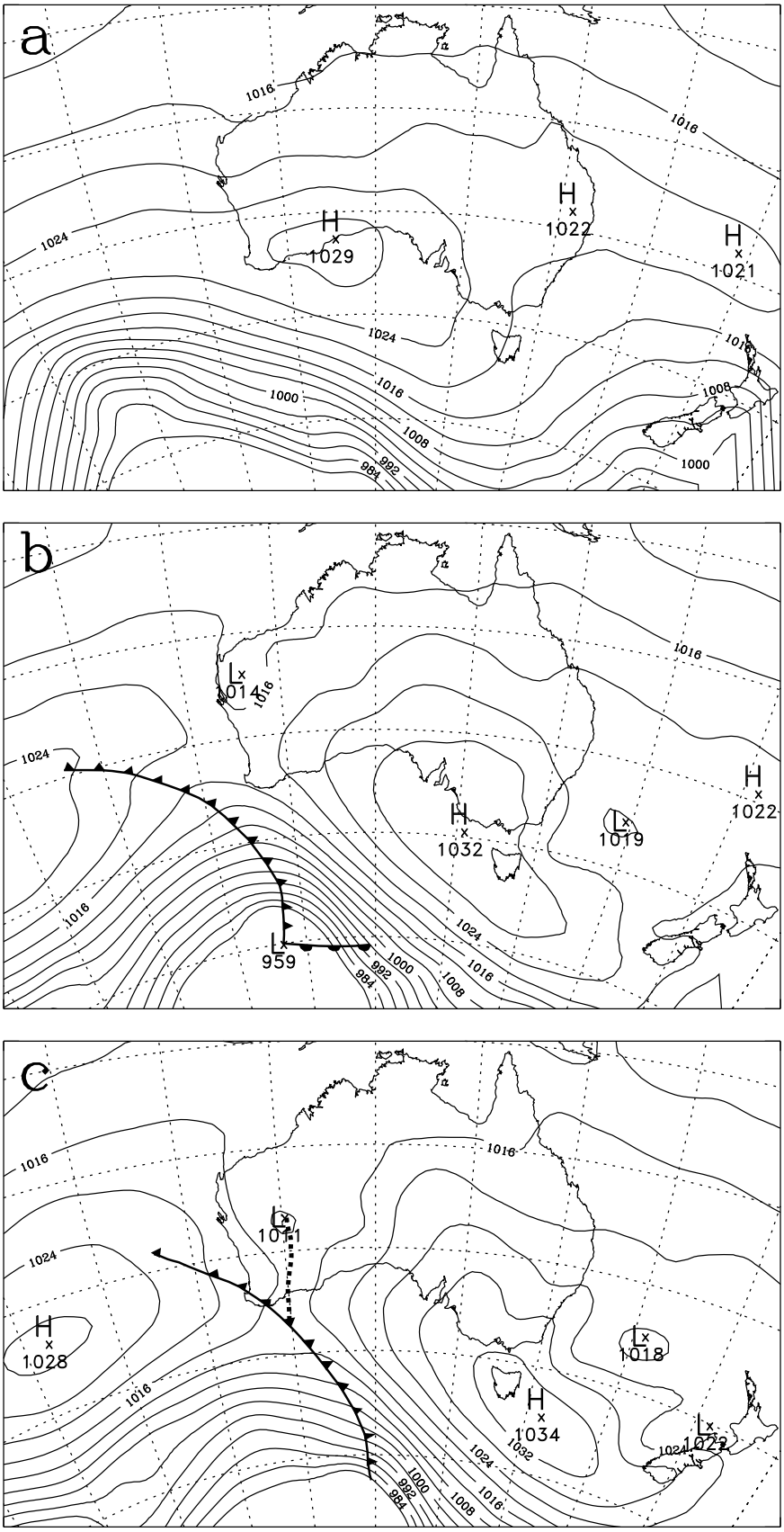

Figure 9. Surface weather chart at (a) 0800 LST (0000 UTC) 12 August 2007, (b) 0800 LST 13 August 2007, and (c) 2000 LST 13 August 2007.

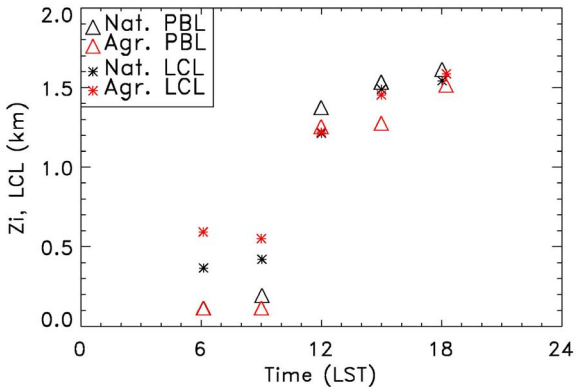

Figure 10. Time evolution of PBL height (triangle) and LCL (asterisk) for 12 August 2007 (red, agriculture; black, native vegetation).

trough (WCT) feature [*Ma et al.*, 2001]. The wind flow associated with the WCT primes the conditions for convective development by inducing a southerly transport of heated, continental air masses east of its axis with a nearly adiabatic lapse rate over southwest Australia. A very deep PBL can develop under such conditions, exceeding the LCL and generating convective clouds. Low-level convergence also occurs due to sea breeze and nocturnal low-level jet interactions. The WCT often exhibits a northwest orientation and the role of WCT in the formation of cloud fields that terminate along the rabbit-proof fence (Figure 3a) is not completely understood.

[13] During BuFex05, the boundary layer development during such an event was sampled on 17–18 December 2005 (Figure 5). Vigorous boundary layer development occurred under the calm conditions accompanying the high-pressure system that was established over southwest Australia (Figure 5a). Surface pressure observations show the development of the WCT during the afternoon hours of 17 December and its establishment over the southwest Australian region by 0800 LST 18 December 2005 (Figure 5b). While the WCT formed during the afternoon hours of 17 December 2005, satellite imagery did not show any substantial cloud development. Further deepening of the WCT occurred during the day on 18 December 2005 in response to heating (Figure 5c) and eventually moved east during the evening hours. While no rainfall was recorded on 18 December 2005, preferential cloud formation did occur over native vegetation during the late afternoon hours (Figure 3b) allowing for analysis of processes that lead to preferential cloud formation, including the role of the WCT.

[14] The diurnal variation of observed PBL heights over the agricultural and native vegetation regions on 17 December 2005 was examined to determine the impact of LCC on the development of the WCT (Figure 6). Note that clear sky conditions existed over both regions allowing for straightforward comparisons of PBL development. Compared to the agricultural area, substantially higher PBL heights occur over the native vegetation during the afternoon hours, very nearly approaching the LCL at 1500 LST (Figure 6). By 1700 LST the PBL height over the agricultural area is approximately the same as that over the native vegetation at 1500 LST, while over the native vegetation, the arrival of the sea breeze caused the decoupling of the mixed layer from the surface. The arrival of the sea breeze in the agricultural region (the Lake King site) occurs at a later time and prior modeling studies show that the difference in time of arrival of the sea breeze between these areas is not related to LCC [*Kala et al.*, 2010].

[15] RAMS simulations for 18 December 2005 show that the structure of the WCT is sensitive to LCC, with the low-pressure core of the WCT feature expanding and the orientation of the southern part becoming more southwesterly when the agricultural clearing is replaced with native vegetation (Figures 7a and 7b). Areas of enhanced PBL heights in both the CLU and PELU scenarios are found to be associated with the simulated WCT pattern in these scenarios (Figures 7d and 7e). Over the regions of enhanced PBL development, the cloud development observed in satellite imagery (Figure 3b) correlates well with the areas of larger PBL heights in the numerical model simulation for the CLU scenario (Figure 7d). When the agricultural land cover is replaced by native vegetation, the region of enhanced PBL development extends farther west (Figure 7e, 7c). Simulations using a higher-resolution 1 km grid over the Lake King area show that when native vegetation occupies areas to the west of the fence, the convective eddies penetrate to substantially higher levels (Figures 7e and 7f), thus increasing the potential for cloud formation to the west of the fence. Even though the PBL heights simulated with the 1 km spacing grid exceeded 4.5 km, simulated eddies did not reach high LCL heights observed on 18 December. Note that the summertime WCT event considered in this study did not produce any precipitation but showed a deeper convective boundary layer over the native vegetation consistent with the analysis of *Huang et al.* [1995] who suggested that conditions are more favorable for cloud development over native vegetation.

3.2. Wintertime Boundary Layer and Convective Development

[16] Boundary layer heights derived from the paired radiosonde releases from August 2007 also show a strong tendency for the PBL heights in the afternoon hours to be higher over the native vegetation areas compared to the agricultural areas (Figure 8a), consistent with the analysis of *Huang et al.* [1995]. The mean difference in PBL heights between the native vegetation and agricultural areas is ~189 m and ~133 m at 1200 and 1500 LST, respectively, both of which are statistically significant at a 95% confidence level. Due to moister boundary layer conditions resulting from frequent frontal passage and rainfall, the LCL was found to be substantially lower during the wintertime. While lower LCL heights were observed over the agricultural area, it did not increase the probability of cloud formation for the majority of the days, since the PBL heights exceeded the LCL on 17 out of 20 days. Aircraft observations of surface energy fluxes do show that sensible heat fluxes were higher over the native vegetation areas (Figure 8b).

[17] The latent heat fluxes over the native vegetation areas do not vary substantially from summer (Figure 4c) to winter (Figure 8c), and rarely exceed 40 W m^{-2}. However, over the agricultural areas, they increase during wintertime, ranging

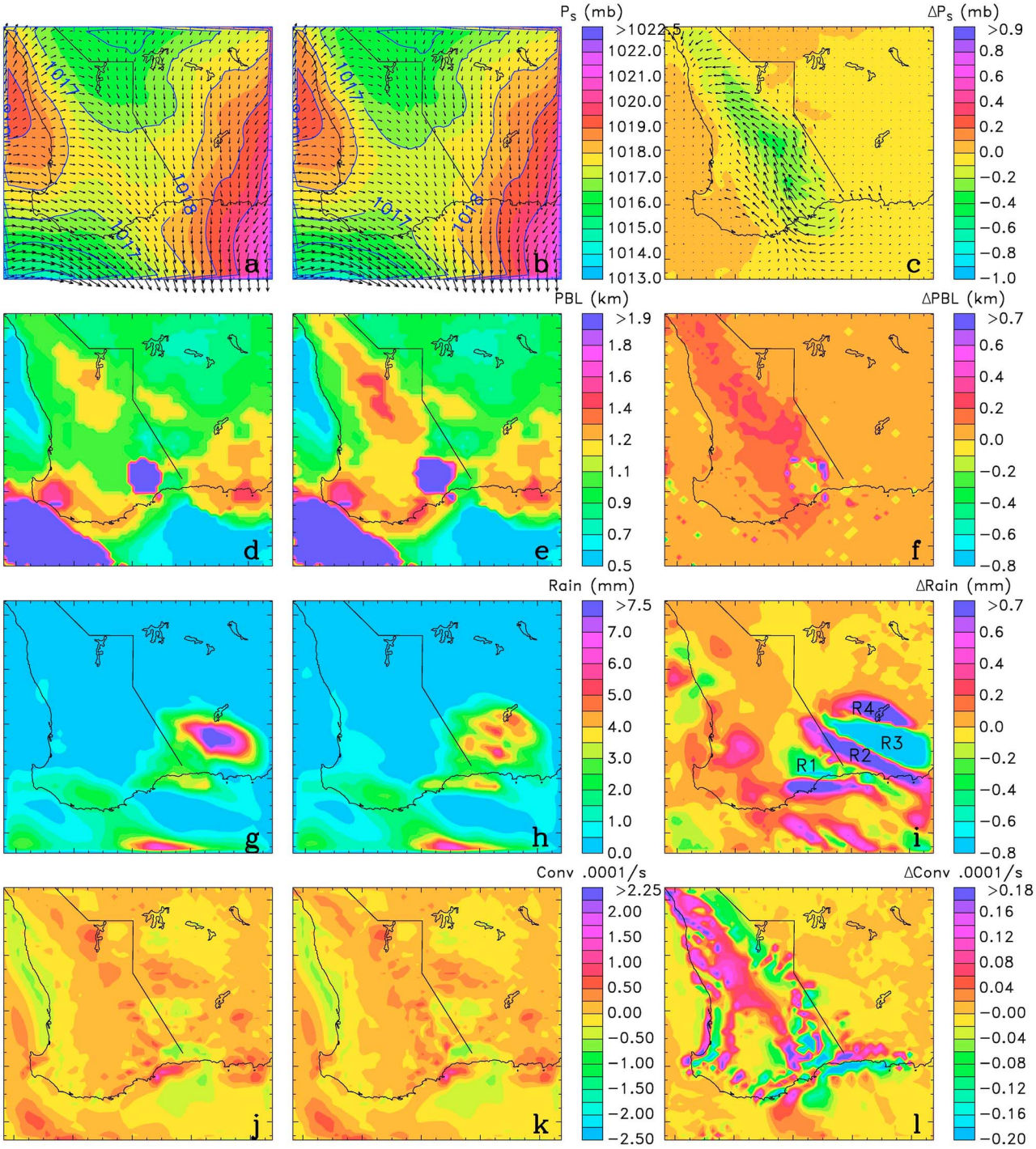

Figure 11. Mean sea level pressure in the (a) CLU and (b) PELU simulations at 1500 LST, 13 August 2007, and (c) the difference between the PELU and CLU simulations. (d, e, and f) Same as Figures 11a, 11b, and 11c but for PBL heights at 1500 LST, 13 August 2007. (g, h, and i) Same as Figures 11a, 11b, and 11c but for 24 h accumulated rainfall at 0000 LST on 14 August 2007. (j, k, and l) Same as Figures 11a, 11b, and 11c but for surface convergence.

between 40 and 80 W m^{-2} (Figure 8c), compared to summertime when they did not exceed 30 W m^{-2}, consistent with the analysis of *Lyons et al.* [1996]. The higher latent heat fluxes over the agricultural areas compared to native vegetation in wintertime are due to both higher rainfall over these regions and the tendency of the nonnative agricultural species to transpire more than the native species, with the latter ones being adapted better to the semiarid conditions.

[18] Development of the WCT also occurs during the wintertime and such an event was sampled during

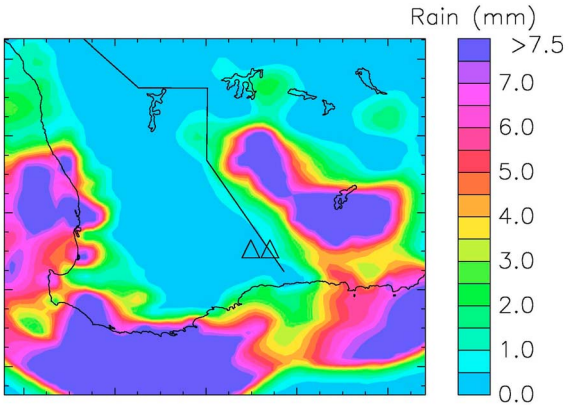

Figure 12. The 24 h accumulated rainfall observation plotted for the grid 2 simulation domain at 0000 LST on 14 August 2007.

12–13 August 2007 (Figure 9). On 12 August 2007, southwest Australia was under the influence of a high-pressure system and easterly flow dominated the region (Figure 9a). A heat low developed in northwestern Australia on 13 August and the associated trough became mobile, bringing rain in the Lake King region during the night (Figure 9b). A cold front that followed the trough brought rainfall to the west coast (Figure 9c). The pattern of boundary layer development was very similar to the WCT event sampled during December 2005. On 12 August the PBL over the native vegetation was consistently higher during the afternoon hours (Figure 10); hence penetration above the LCL is more likely over the native vegetation.

[19] After 1200 LST, the PBL height over the agricultural region was slightly below the LCL while it exceeded the LCL in the native vegetation areas. Satellite observations showed a persistence of fair weather cumulus over the native vegetation in the afternoon while clearing is found over the agricultural area. Another feature observed in both the numerical simulation and the satellite observations (Figure 3c) is the formation of clouds along the zone of low-level convergence as the southerly sea breeze flow collides with the northwesterly flow to the east of the WCT. In the numerical simulations, this convergence zone is strengthened to the west of the fence when the agriculture clearing is eliminated, producing deeper nocturnal convection (not shown) in the same region.

[20] On 13 August, a trough developed over the southwest Australian region, and similar to summertime, the trough development is indeed impacted by the land cover (Figures 11a, 11b, and 11c). The core region of the trough occupies a larger area when there is native vegetation to the west of the rabbit-proof fence (Figure 11b). However, the impact of the land cover on the daytime evolution of the trough is less drastic compared to that simulated for the summertime case. PBL development in excess of 1 km is observed over both native and agricultural regions, with higher PBLs observed over native vegetation (Figure 11d, 11e, and 11f). Satellite imagery at 1500 LST shows active convection over native vegetation associated with the WCT (Figure 3c). However, unlike the summer case, the winter situation is more complicated due to the presence of convection ahead of the cold front approaching the southwest coastal region.

[21] Similar to observations, numerical model simulations show higher PBLs to the east of the fence for the current LCC (Figure 11e). When the agriculture land cover is replaced by native vegetation as simulated by the PELU scenario, enhanced heating and associated deepening of the trough leads to changes in the wind field along a band approximately parallel to and offset to the west of the vermin-proof fence (Figure 11c). Areas of enhanced PBL height and surface convergence (Figures 11f and 11l) in the PELU scenario are well correlated to the wind and surface pressure anomalies (Figure 11c). During the nighttime when the trough moves east, convection is initiated along convergence zones associated with its low-level circulation patterns. Comparison of RAMS simulated rainfall for the CLU conditions (Figure 11j) to gridded rainfall analysis (Figure 12) show that the simulation underestimates rainfall over the ocean areas. However, note that the gridded rainfall analysis is based on point observations that are sparse over oceanic regions and also over some of the adjacent land area. Over land, the simulation captures the general pattern of rainfall better, but underestimates the northward extend of rainfall to the east of the vermin-proof fence and also the accumulated precipitation amounts along the western and southern coastal regions. The simulated rainfall pattern is substantially altered under PELU conditions, with a general increase in rainfall found to the west of the vermin-proof fence except for a localized region of decreased precipitation (R1 in Figure 11i). The majority of the areas of increased rainfall to the west of the fence and the southern coast (Figure 11i) coincide with regions of enhanced convergence, with the percentage increase in rainfall in the PELU scenario exceeding 100% (not shown) over some of these areas. Note that other modeling studies, both case studies [*Kala et al.*, 2011] and seasonal simulations [*Pitman et al.*, 2004] also report precipitation increases for the PELU scenario. To the east of the fence, PELU results in three alternating bands of positive and negative rainfall anomalies (R2, R3, and R4 in Figure 11i). This is because the simulated spatial distribution of precipitation for the PELU scenario exhibits three distinct local maxima of accumulated precipitation as opposed to one distinct maximum found for CLU conditions.

4. Discussion

[22] The observational and numerical model analysis shows that while the structure and orientation of WCT produce large-scale conditions that are conducive to preferential cloud formation over the native vegetation during summer, land cover modulates the boundary layer development even under the influence of the WCT. While the spatial orientation of the WCT is often similar to that of the rabbit-proof fence, it is unlikely that the areas of enhanced boundary layer development will always relate closely to the areas separated by the fence. Numerical modeling simulations show that the structure of the WCT itself is altered by LCC and enhanced boundary layer development is extended to the west of the fence in the absence of the land clearing. This shows that the observed termination of summertime cloud fields along the fence (Figure 3b) is

potentially related to the differences in land use in the vicinity of the fence.

[23] Depending on the large-scale distribution of boundary layer moisture, as shown by the radiosonde observations on 17 December 2005 (Figure 6), enhanced PBL development over the native vegetation increase the probability of the PBL top exceeding the LCL, causing cloud fields to form exclusively over the native vegetation. Examination of satellite imagery in conjunction with surface meteorological analysis shows similar, preferential cloud formation over native vegetation area during other WCT events (for example, 3 January 1999; Figure 3a).

[24] In the context of the decreasing precipitation trends reported for this region, it is relevant whether such differences in cloudiness would impact rainfall over the agricultural areas. While the summertime case considered in the present study (see section 3.1) did not produce precipitation, rainfall observations associated with a prior summertime WCT event that occurred on 10 February 1999, shows that clouds forming preferentially along the northern part of the fence resulted in the only rainfall event in that region for that month. Therefore, it is probable that without the LCC and the resulting extension of the WCT, cloud fields farther west could increase austral spring and summer precipitation along a zone parallel to the fence. The relative narrowness of the area impacted, combined with the spotty nature of precipitation associated with scattered thunderstorms, could be the reason why the observations do not show a statistically significant trend of rainfall decrease during the austral spring and summer [*Williams*, 1991; *Narisma and Pitman*, 2003], in contradiction to numerical models which show such a trend in response to LCC [*Narisma and Pitman*, 2003].

[25] Prior studies [*Narisma and Pitman*, 2003; *Pitman et al.*, 2004] suggested that the following mechanisms may be responsible for decreased rainfall associated with clearing of native vegetation: (1) Decrease in physical evaporation and transpiration, and (2) Decrease in moisture convergence causing a deficit in rainfall in regions adjacent to the coast, while an increase in moisture convergence leads to an increase in rainfall farther inland. *Pitman et al.* [2004] concluded that the change in moisture convergence, which, in turn, is due to decreased roughness, is the primary cause for alterations in rainfall. Results from the present study support these mechanisms. Aircraft observations show that during the wetter winter season, latent heat fluxes over areas of native vegetation are lower than over the agricultural areas. Furthermore, the latent heat fluxes over the native vegetation do not vary substantially between the winter and summer seasons, indicating that the transpiration from the native vegetation is less sensitive to soil moisture availability. The deep rooted native vegetation has access to the underground aquifer whereas the shallow rooted agricultural crops are reliant on near-surface soil moisture and hence their greater sensitivity to soil moisture. One of the consequences of replacing native vegetation with agricultural crops is the removal of this link between the underground aquifer and the atmosphere.

[26] In general, the response of the numerically simulated surface convergence (Figure 11l) and moisture convergence (not shown, but the pattern is very similar to mass convergence) fields to clearing of native vegetation is similar to that reported by *Pitman et al.* [2004]. However, unlike *Pitman et al.* [2004], localized regions of increased (decreased) mass and moisture convergence is also found in inland (coastal) areas. This difference is because *Pitman et al.* [2004] utilized monthly averages, while our analysis is made for particular case days.

[27] To the west of the fence, areas of decreased (increased) precipitation (Figures 11g–11i) in response to clearing of native vegetation are generally associated with areas of decreased (increased) mass convergence (Figures 11j–11l). To the east of the fence, numerical simulations do not show substantial changes in surface convergence except near the coast. However, there are substantial changes in the rainfall pattern (Figures 11g–11i) with a "bull's -eye" pattern occurring under the CLU scenario as opposed to a more widespread pattern of rain with multiple maxima for the PELU scenario. While the differences in rainfall to the west of the fence are related to changes in surface convergence, the mechanism responsible for rainfall changes to the east of the fence is not clear and requires further study.

[28] Note that while *Pitman et al.* [2004] attributes the differences in surface convergence between the CLU and PELU scenarios to interactions of surface winds with altered surface roughness regimes, the current study found specific changes to synoptic-scale features caused by land use change are also important. Development of the heat lows, which played a dominant role in events that occurred on the case study days, were substantially impacted by clearing of native vegetation to the west of the fence. Replacement of native vegetation in the cleared areas intensified the heat lows found on both case days (Figures 7a–7c and Figures 11a–11c). Whereas the smaller, wintertime differences in PBL heights between the agricultural and native vegetation areas did not increase the probability of cloud formation on the majority of the days (see section 3.2), enhanced heating over the native vegetation areas did contribute to intensification of the wintertime heat low. The anomalies in wind fields associated with the intensification of the pressure system for the wintertime case day coincides well with anomalies of PBL height, precipitation and surface convergence. This suggests that in addition to the direct role of the altered surface roughness, modifications to development and evolution of mesoscale and synoptic-scale features such as pressure systems, atmospheric fronts, etc., caused by land use change also need to be considered. A recent case study by *Kala et al.* [2011] that found clearing of native vegetation reducing rainfall produced by the passage of a frontal system further supports this conclusion and the need for studying the impact of land use change on specific mesoscale and synoptic systems relevant to the region.

[29] The maximum differences in accumulated rainfall between the two land cover scenarios were found to be substantially higher in the simulations with smaller grid spacing (16, 4, and 1 km). The inability of coarser grids utilized in prior modeling analyses [*Narisma and Pitman*, 2003; *Pitman et al.*, 2004] to suitably resolve small-scale convergence features could be the reason for the conclusion that the resulting pattern of precipitation decrease to be dominated by the effects of changes in surface roughness.

[30] Note that the analysis conducted in this study is based on the WTC events that coincided with the BuFex field

campaign. This constrains the numerical modeling analysis to select case study days and thus may not be a representative sampling of the WTC phenomenon. The sensitivity of WTC evolution to LCC found in the numerical experiments should be viewed in this context, and further numerical experiments need to conducted in order to determine its variability.

5. Conclusions

[31] Analysis of radiosonde and aircraft observations, characterizing PBL development and surface energy fluxes as a function of land cover and season, along with numerical modeling analysis is used to show that in southwest Australia: (1) the west coast trough (WCT), which often forces summertime convection, is impacted by LCC causing cloud fields to preferentially terminate along the rabbit-proof fence; (2) enhanced PBL heights over the native vegetation increase the probability of cloud formation by allowing surface air to reach the LCL; (3) the LCC also impacts the WCT during the winter season and the tendency for higher PBLs over native vegetation persists during this period; and (4) while the most visible effect of LCC on regional climate is the cloud fields that terminate along the fence, the primary cause for rainfall decrease in this region is due to changes in low-level convergence, caused by alteration of both WCT dynamics and aerodynamic roughness. This study identifies some of the processes through which landscape influences weather and climate. It suggests that the impact of LCC on atmospheric processes should be a consideration for land management policies in the regions around the globe where significant land clearing for agriculture purposes is occurring.

[32] **Acknowledgments.** This research is supported by the National Science Foundation grant ATM-0523583 and the Australian Research Council Discovery Program (project DP0664515). The radiosonde observations were acquired using the National Center for Atmospheric Research MGAUS, and the aircraft observations were carried out by Airborne Research Australia, both of which were supported by the NSF and ARC Discovery Program. The authors are thankful to Pandora Hope for permitting the use of graphic shown in Figure 2. The authors also thank Tokio Kikuchi for providing the satellite imagery used in Figures 3a and 3c. The manuscript was, as usual, very ably edited by Dallas Staley.

References

Bates, B., P. Hope, B. Ryan, I. Smith, and S. P. Charles (2008), Key findings from the Indian Ocean Climate Initiative and their impact on policy development in Australia, *Clim. Change*, *89*, 339–354, doi:10.1007/s10584-007-9390-9.

Bolton, D. (1980), The computation of equivalent potential temperature, *Mon. Weather Rev.*, *108*, 1046–1053, doi:10.1175/1520-0493(1980)108<1046:TCOEPT>2.0.CO;2.

Cai, W., and I. G. Watterson (2002), Modes of interannual variability of the Southern Hemisphere circulation simulated by the CSIRO climate model, *J. Clim.*, *15*, 1159–1174, doi:10.1175/1520-0442(2002)015<1159:MOIVOT>2.0.CO;2.

Cotton, W. R., et al. (2003), RAMS 2001: Current status and future directions, *Meteorol. Atmos. Phys.*, *82*, 5–29, doi:10.1007/s00703-001-0584-9.

Harrington, Y. Y., T. Reisin, W. R. Cotton, and S. M. Kreidenweis (1999), Cloud resolving simulations of Arctic stratus. Part II: Transition-season clouds, *Atmos. Res.*, *51*, 45–75, doi:10.1016/S0169-8095(98)00098-2.

Hope, P. K. (2006), Projected future changes in synoptic systems influencing southwest Western Australia, *Clim. Dyn.*, *26*, 765–780, doi:10.1007/s00382-006-0116-x.

Huang, X., T. J. Lyons, and R. C. G. Smith (1995), The meteorological impact of replacing native perennial vegetation with annual agricultural species, *Hydrol. Processes*, *9*, 645–654, doi:10.1002/hyp.3360090512.

IOCI Panel (2002), Climate variability and change in south west Western Australia, report, Indian Ocean Clim. Initiative, East Perth, WA, Australia.

Kala, J., T. J. Lyons, D. J. Abbs, and U. S. Nair (2010), Numerical simulation of the impacts of land-cover change on a southern sea-breeze in south-western Western Australia, *Boundary Layer Meteorol.*, *135*, 485–503, doi:10.1007/s10546-010-9486-z.

Kala, J., T. J. Lyons, and U. S. Nair (2011), Numeral simulations of the impact of land-cover change on cold fronts in south-west Western Australia, *Boundary Layer Meteorol.*, *138*, 121–138, doi:10.1007/s10546-010-9547-3.

Lyons, T. J. (2002), Clouds prefer native vegetation, *Meteorol. Atmos. Phys.*, *80*, 131–140, doi:10.1007/s007030200020.

Lyons, T. J., P. Schwerdtfeger, J. M. Hacker, I. J. Foster, R. C. G. Smith, and H. Xinmei (1993), Land-atmosphere interaction in a semiarid region: The Bunny Fence Experiment, *Bull. Am. Meteorol. Soc.*, *74*, 1327–1334, doi:10.1175/1520-0477(1993)074<1327:LIIASR>2.0.CO;2.

Lyons, T. J., R. C. G. Smith, and H. Ximmei (1996), The impact of clearing for agriculture on the surface energy budget, *Int. J. Climatol.*, *16*, 551–558, doi:10.1002/(SICI)1097-0088(199605)16:5<551::AID-JOC25>3.0.CO;2-9.

Lyons, T. J., L. Fuqin, J. M. Hacker, W.-L. Cheng, and H. Xinmei (2001), Regional turbulent statistics over contrasting natural surfaces, *Meteorol. Atmos. Phys.*, *78*, 183–194, doi:10.1007/s703-001-8172-0.

Ma, Y., T. J. Lyons, and J. A. Blockley (2001), Surface influences on the Australian west coast trough, *Theor. Appl. Climatol.*, *68*, 207–217, doi:10.1007/s007040170046.

Narisma, G. T., and A. J. Pitman (2003), The impact of 200 years of land cover change on the Australian near-surface climate, *J. Hydrometeorol.*, *4*, 424–436, doi:10.1175/1525-7541(2003)4<424:TIOYOL>2.0.CO;2.

Nicholls, N. (2010), Local and remote causes of the southern Australian autumn-winter rainfall decline, *Clim. Dyn.*, *34*, 835–845, doi:10.1007/s00382-009-0527-6.

Pitman, A. J., G. T. Narisma, R. Pielke, and N. J. Holbrook (2004), The impact of land cover change on the climate of southwest Western Australia, *J. Geophys. Res.*, *109*, D18109, doi:10.1029/2003JD004347.

Pittock, A. B. (1983), Recent climate change in Australia: Implications for a CO_2-warmed Earth, *Clim. Change*, *5*, 321–340.

Ray, D. K., U. S. Nair, R. M. Welch, Q. Han, J. Zeng, W. Su, T. Kikuchi, and T. J. Lyons (2003), Effects of land use in southwest Australia: 1. Observations of cumulus cloudiness and energy fluxes, *J. Geophys. Res.*, *108*(D14), 4414, doi:10.1029/2002JD002654.

Timbal, B., and J. M. Arblaster (2006), Land cover change as an additional forcing to explain the rainfall decline in the south west of Australia, *Geophys. Res. Lett.*, *33*, L07717, doi:10.1029/2005GL025361.

Walko, R. L., et al. (2000), Coupled atmosphere-biophysics-hydrology models for environmental modeling, *J. Appl. Meteorol.*, *39*, 931–944, doi: 10.1175/1520-0450(2000)039<0931:CABHMF>2.0.CO;2.

Williams, A. (1991), Climate change in southwest of western Australia, B.Sc. (Hons) thesis, 116 pp., Environ. Sci., Murdoch Univ., Murdoch, West. Aust., Australia.

J. M. Hacker, Airborne Research Australia, Flinders University, Adelaide, SA 5001, Australia.

J. Kala and T. J. Lyons, School of Environmental Sciences, Murdoch University, South Street, Murdoch, 6150 WA, Australia.

U. S. Nair and Y. Wu, Earth System Science Center, University of Alabama in Huntsville, 320 Sparkman Dr., Huntsville, AL 35805, USA. (nair@nsstc.uah.edu)

R. A. Pielke Sr., Cooperative Institute for Research in Environment Sciences, University of Colorado at Boulder, Boulder, CO 80309, USA.